

## Bio-optical properties of the San Jorge Gulf (Argentina)

Gabriela Williams<sup>1</sup>, Pierre Larouche<sup>2</sup>, Ana I. Dogliotti<sup>3</sup>

<sup>1</sup> Centro para el Estudio de Sistemas Marinos (CESIMAR), CONICET, Puerto Madryn Argentina

<sup>2</sup> Maurice Lamontagne Institute, Fisheries and Oceans Canada, Mont-Joli, Quebec, Canada G5H 3Z4

<sup>3</sup> Instituto de Astronomía y Física del Espacio (IAFE), CONICET/UBA, Argentina

The San Jorge Gulf is a region of high ecological importance where several industrial fisheries exploit species like hake (*Merluccius hubbsi*), the Argentine red shrimp (*Pleoticus muelleri*) and the Patagonian scallop (*Zygochlamys patagonica*). In this region phytoplankton is known to grow in patches which are often related to bathymetric or oceanographic features such as capes, upwelling and frontal areas that drive the renewal of nutrients in the surface layer. Although remote sensing is a key tool to monitor such a large ecosystem it is necessary to validate operational ocean color algorithms and build adapted ones if needed. Inherent optical properties and chlorophyll-a in the surface layer of the area were measured in February 2014. For this set of data, a match-up analysis showed a good performance of the MODIS OC3v5 algorithm ( $r^2=0.89$ , RPD=25.77%, n=7). The overestimation could be related to the dominance of CDOM (>48%) to the total non-water absorption coefficient. Finally, the strong spatial variability of the measured parameters was related to a tidal front in the south of the gulf.

### 1. Introduction

Remote sensing of ocean colour focused primarily on the retrieval of chlorophyll-a (Chl-a) concentrations in the global oceans. Water colour is determined by the inherent optical properties (IOPs, 1), and chlorophyll is just one of the active components that determine the IOPs. Therefore Chl-a can be determined only with a larger uncertainty from ocean-colour remote sensing than the inherent optical properties themselves. Variations in IOPs are clear indications of changes in water mass or water constituents. Increased knowledge of the spatial and temporal variability of the optical properties can optimize the use of ocean color remote sensing and eventually provide improved and reliable products related to the biogeochemistry of the oceans (2).

The San Jorge gulf (SJG), located in the Argentine Patagonian region around 46°S (Fig. 1), has a significant biological importance where several economic activities are developed, including two industrial fisheries: hake (*Merluccius hubbsi*, Marini, 1933) and Argentine red shrimp (*Pleoticus muelleri*, Bate, 1888) and the Patagonian scallop (*Zygochlamys patagonica*). Phytoplankton is at the base of the oceanic food web and through its production of organic matter fuels marine ecosystems, thus making it a valuable indicator to characterize their state. In the southern SJG, it has been observed that fisheries are linked to a tidal front (3, 4, 5, 6, 7, 8, 9) that has been shown to be associated to relatively high chlorophyll-a level throughout spring and summer, which can be detected by ocean color sensors (10, 11, 5, 12, 9). In turn, in situ measurements indicated high surface Chl-a concentrations (14.00 mg.m<sup>-3</sup>) in spring and fall (4). However, despite the ecological and biogeochemical relevance of the SJG front, there are no records of IOPs measurements in the study area.

The aim of the present work is thus to analyse the first bio-optical measurements collected during an oceanographic cruise carried out in summer in SJG. Data is analysed to (1) determine the optical characteristics of the main seawater components (i.e., phytoplankton, detritus, and coloured dissolved organic matter) and (2) to assess the quality of chlorophyll-a concentration estimations by remote sensing of ocean-colour using in-situ data.

## 2. Data and Methods

### 2.1 Study area and Sampling

The SJG, a semi-open basin with an extension of 39,340 km<sup>2</sup>, is located between 45°S (Cape Dos Bahias) and 47°S (Cape Tres Puntas), and between 65°30'W and the coast of Argentine Patagonia (Fig. 1).

There are no rivers flowing into the gulf and precipitations are scarce (average: 233 mm.yr<sup>-1</sup>). Sediments from the central basin of the gulf, a depositional environment, are dominated by fine silt and rich in organic carbon derived from seasonally high phytoplanktonic primary production in the upper layer of the water column (6, 13, 14), while continental input is negligible. The so-called Patagonian Shelf Water, including that of SJG, is a mixture of subantarctic waters from the Cape Horn Current and low-salinity waters from the Magellan Plume.

The data were collected during the MARES (MARine ecosystem health of the San Jorge Gulf: Present status and RESilience capacity) expedition in the summer 2014 (between January, 29 and February, 15) in the continental margin and the SJG areas (Figure 1). It was operationally integrated by 3 legs. During the first leg the water column in the continental margin (“blue hole”) was sampled at 5 stations. The second leg included both, a high resolution data acquisition survey in the southern frontal zone of the SJG (F1-F10 stations, Figure 1) and a time series sampling (15 stations) at a fixed site located in the center of the Gulf (SFx stations, Figure 1). There were 16 stations in the third leg covering the whole area of the SJG (Figure 1). At each station, surface water samples were collected with a clean container (Niskin bottles) and analyzed for absorption properties and Chl-a concentration. CTD profiles indicated that the central area of the Gulf appears highly stratified and stable in the first 40 m while the northeast and southeast areas of the Gulf are mixed (Coriolis II cruise, not published data, 15). Therefore, the near-surface data measured in the study area should represent the optical parameters within the first optical depth. All processing protocols described later are compliant with the recommendations for satellite ocean color sensor validation by Mitchell et al. (16).

### 2.2 Determination of particle and CDOM absorption and chlorophyll-a concentration.

Samples of seawater were filtered on board onto GFF glass-fibre-filters, at dim light and low pressure (0.35 kPa). Filters were stored at -80°C until analysis.

Optical density of the total particulate material was measured between 350 and 750 nm to obtain total particulate absorption ( $a_p(\lambda)$ ) using a double beam Shimadzu UV-210A spectrophotometer following the quantitative filter technique (17, 18, 19).

The absorption coefficient of NAP,  $a_{NAP}(\lambda)$ , was measured after pigment bleaching with 95% methanol (MeOH) (19). According to the results from Babin and Stramski (20), aquatic particles generally show no absorption in the near-infrared, so the final estimates of  $a_p(\lambda)$  and  $a_{NAP}(\lambda)$  were obtained by subtracting the averaged  $a_p(\lambda)$  and  $a_{NAP}(\lambda)$  values over 790–800 nm from all

the measured spectral values  $a_p(\lambda)$  and  $a_{NAP}(\lambda)$ , respectively. The phytoplankton absorption coefficient  $a_{ph}(\lambda)$  was obtained from the following equation:

$$a_{ph}(\lambda) = a_p(\lambda) - a_{NAP}(\lambda)$$

Coloured dissolved organic matter (CDOM) optical density was measured in filtered water samples (0.2  $\mu\text{m}$  Anotop filters, acid pre-washed) between 250 and 800 nm using a simple beam spectrophotometer (HP8452 diode array).

Chl-a was extracted with 90% acetone and measured with a *Turner design 10-AU* fluorometer according to Strickland and Parsons (21).

### 2.3 Remote sensing data

Moderate-Resolution Imaging Spectroradiometer (MODIS) Aqua Level-2 files were acquired for the study area (Fig. 1) from the NASA ocean color web site ([oceancolor.gsfc.nasa.gov](http://oceancolor.gsfc.nasa.gov)) for the dates when concurrent in-situ Chl-a measurements were available. The standard Chl-a product derived from the OC3v5 algorithm (OC3M updated version after the 2009 reprocessing) were used.

In order to define the temporal coincidence between satellite and in-situ measurements, different temporal windows were analyzed ( $\pm 3$ ,  $\pm 6$ ,  $\pm 12$  and  $\pm 20$  h). Values of Chl-a used in the match-up were the mean of all unmasked pixels within a  $3 \times 3$  pixel box centered on the in-situ target. Satellite Chl-a was excluded when more than 50% of marine pixels within this box were masked or when the coefficient of variation of the valid marine pixels exceeded 0.20.

### 2.4 Testing MODIS standard Chl-a algorithm

With the goal of evaluating the performance of the OC3v5 algorithm, linear regression analyses were carried out between the in-situ chlorophyll-a concentration, and the satellite product. The statistical parameters used for these evaluations were the mean relative percentage difference (RPD), the mean absolute percentage difference (APD) and the root mean square error (RMSE) between satellite-derived (sat) and measured (in-situ) Chl-a. These parameters are defined as:

$$RPD = \frac{1}{n} \sum_{n=1}^N ((X_{sat} - X_{situ}) / X_{situ}) \times 100 \quad (2)$$

$$APD = 1/n \sum_{n=1}^N |(X_{sat} - X_{situ}) / X_{situ}| \times 100 \quad (3)$$

$$RMSE = \sqrt{1/n \sum_{n=1}^N ((X_{sat} - X_{situ}) / X_{situ})^2} \times 100 \quad (4)$$

Where, X is Chl-a, and n is the number of pairs of data (match-ups) analyzed. The slope, intercept and the determination coefficient ( $r^2_{SMA}$ ) were calculated following a type II linear regression model, Standard Major Axis (SMA) (22,23). Log transformations were applied to satellite and in-situ chlorophyll-a data since the bio-optical data have a log-normal distribution

(24). The linear-transformed root mean square error (rmse-L) (25) and the root mean square log-error (RMSE-log.), were calculated using the following equations:

$$rmse - L = 0.5 \left[ (10^{+RMSE_{log}} - 1) + (1 - 10^{-RMSE_{log}}) \right] \quad (5)$$

Where

$$RMSE_{log} = \sqrt{1/n \sum_{n=1}^N (\log_{10}(Chla_{sat}) - \log_{10}(Chla_{situ}))^2} \quad (6)$$

### 3. Results

#### 3.1 Spatial variability

At the end of summer (February) the mean concentration of chlorophyll was  $1.34 \pm 0.66 \text{ mg.m}^{-3}$ . The highest relative concentrations were measured at stations localized close to the southeast (G13, F1 and F10) and southwest coasts (G01), see locations in Fig. 1. Stations with concentrations less than  $2 \text{ mg.m}^{-3}$  were located mainly in the northern area. These results are consistent with the spatial distribution of the chlorophyll-a satellite image shown in Figure 1b (MODIS/Aqua image from February 12, 2014).

The mean value of  $a_{CDOM(440)}$  was  $0.13 \pm 0.11 \text{ m}^{-1}$  with minimum values in stations G15 and G12 located in the north and south of the mouth of the gulf, respectively. High values were observed in the north area (G5-G7 and G16, Figure 2b)

The mean value of  $a_p$  was  $0.09 \pm 0.03 \text{ m}^{-1}$ , the highest values were recorded close to the southern coast (G01, G10), in the south (G9, G11 and F8) and at station SF8 (Fig. 2c).

The mean value of  $a_{NAP}$  was  $0.03 \pm 0.02 \text{ m}^{-1}$ . In the south and north, values were between  $0.02$ - $0.04 \text{ m}^{-1}$ . The maximum values were measured in the south at stations G10 and G11 (Fig. 2d).

The mean value of  $a_{ph}$  was  $0.06 \pm 0.03$ . Relatively high values were located on the southwest coast (G01), in the south (F8) and at station G14. In general the minimum values were located in the southeastern region (Fig. 2e).

#### 3.2 Absorption budget

Unfortunately, due to a storage problem of the CDOM samples, only eight stations met the condition of having simultaneous data of  $a_{ph}$ ,  $a_{CDOM}$  and  $a_{NAP}$ . Figure 3 shows the absorption budget at the seven MODIS wavelengths. The data shows that the total non-water absorption coefficient is clearly dominated by CDOM at all wavelengths in the San Jorge gulf (>48%).

#### 3.3 Particle absorption spectra

The particle absorption spectra ( $a_p(\lambda)$ ) measured in the San Jorge gulf show two obvious absorption peaks around 440 and 675 nm (Fig. 4a). Both these peaks clearly results from higher relative absorption by phytoplankton pigments in the two spectral ranges of 410–530 and 630–700 nm (Fig. 4b). On the other hand, NAP dominates the particle absorption budget at higher wavelengths (>700 nm) and between 540-630 nm.

The regressions between  $a_{\text{ph}}(440)$ ,  $a_{\text{ph}}(675)$ , and Chl-a show significant correlations, especially between  $a_{\text{ph}}(675)$  and Chl-a ( $r^2 = >0.50$ , Figure 5a and b). In the same way the regressions between  $a_{\text{CDOM}}(440)$  and  $a_{\text{ph}}(440)$  and  $a_{\text{CDOM}}(440)$  and  $a_{\text{ph}}(675)$  also shows significant correlations ( $r^2 > 0.48$ , Figure 5c and d).

### 3.4 Chl-a in situ vs. remote sensing match-up analysis

The total number of surface in-situ Chl-a data collected during the oceanographic cruise was 24. Due to cloud cover, quality and the broader temporal coincidence criteria used ( $\pm 20$  h), the maximum number of match-ups was 18. These data covered a range of in-situ Chl-a values from 0.29 to 2.70  $\text{mg}\cdot\text{m}^{-3}$ , while satellite-derived values ranged between 0.4 and 2.63  $\text{mg}\cdot\text{m}^{-3}$ . Table 3 shows that for a  $\pm 20$ h time window, the APD was not very good (APD=50.4%). Narrowing the time window highly improved the statistics with an APD value of 19.5% for a  $\pm 3$ h time window. This is due to the high spatial variability of chlorophyll-a concentration found (Figures 1b and 2a).

## Discussion and conclusions

In this work it was possible to describe for the first time the spatial distribution of light absorption properties in the surface layer of the SJG. There was a large spatial variability of the measured parameters.

The absorption budget suggests that the SJG corresponds to Case 2 waters (26, 27) as it is dominated by CDOM absorption. Even though only 2 of the 7 match-ups had CDOM data, the high correlation between CDOM and phytoplankton absorption at 440 and 675 nm explains the good performance of the MODIS OC3v5 algorithm. While co-variation suggest that CDOM probably results from the degradation of phytoplankton cells and other organic particles, future analysis of the  $a_{\text{CDOM}}(\lambda)$  spectra will try to better define its origin. In line with our results, previous studies in this region have shown that the surface concentration of dissolved organic carbon was higher than at depths greater than 10 m ( $78 \pm 7\mu\text{M}$ , 15). Also, sediments from the central basin of the gulf are dominated by fine silt and are rich in organic carbon derived from seasonally high phytoplanktonic primary production in the upper layer of the water column (6, 13, 14).

Our observations of positively biased OC3M Chl-a estimates relative to coincident in situ measurements are consistent with previous studies that have evaluated the performance of ocean color algorithms in several regions of the world (28, 29, 30). The assessment of the MODIS-Aqua chlorophyll-a algorithms in optically complex coastal and shelf regions has shown that OC3M has a good performance even in cases when Chl-a and CDOM were not related (29, 30). Unlike those complex coastal and shelf regions, there are no rivers flowing into the SJG and therefore the continental input is negligible (6, 13, 14). We thus propose that seasonal tidal fronts in the SJG (10, 11, 5, 12, 9) drive the spatial and temporal variability of its bio-optical properties. The relationships between  $a_{\text{ph}}(\lambda)$  and Chl-a and  $a_{\text{ph}}(\lambda)$  and CDOM will be further analyzed in seasonal studies assessing satellite standard algorithms in San Jorge gulf along with the amount and composition of the total suspended material (TSM).

## Acknowledgment

The authors thanks the Ocean Biology Processing Group (Code614.2) at the GSFC, Greenbelt, MD20 771, for the distribution of the ocean color data. The project was supported by grants

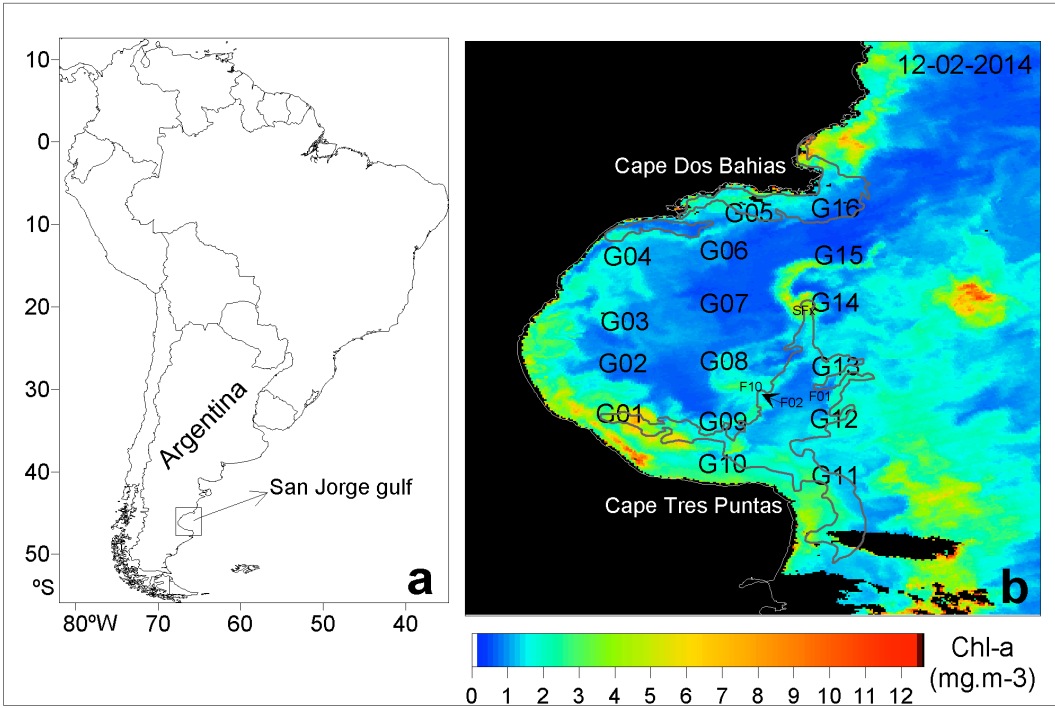
received from the Consejo Nacional de Investigaciones Científicas y Técnicas (PIP 112 20120100350), the Agencia Nacional de Promoción Científica y Tecnológica (PICT 2013-0687), MARES project and Bec.AR program. We thank Juan Ignacio Gossn and Guillermo Ibañez for their help with sampling, Valerie for chlorophyll-a data measurement and Vivian Lutz, Guillermina Ruiz and Valeria Segura for helping with the absorption measurements.

## References

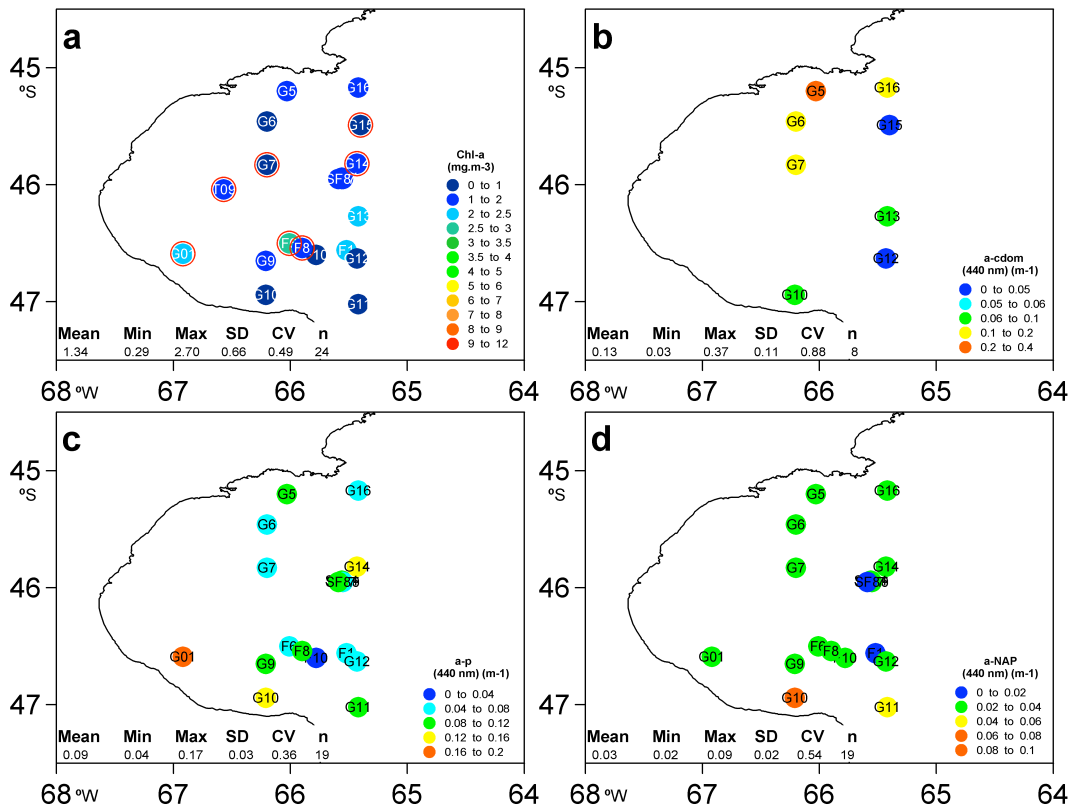
1. R. W. Preisendorfer, "Hydrologic optics". (Vol. I. Introduction, U. S. Department of Commerce National Oceanic and Atmospheric Administration, Environment Research Laboratory, Honolulu, 218 p, 1976).
2. International Ocean Colour Coordinating Group (IOCCG), Remote sensing of inherent optical properties: Fundamentals, tests of algorithms, and applications, (In Z. P. Lee (Ed.), IOCCG Rep. 5, Dartmouth, N. S., Canada, 2006).
3. R. Akselman, Estudios ecológicos en el golfo San Jorge y adyacencias (Atlántico Sudoccidental). Distribución, abundancia y variación estacional del fitoplancton en relación a factores físico-químicos y la dinámica hidrológica, PhD. thesis, Universidad de Buenos Aires, Facultad de Ciencias Exactas y Naturales, Argentina (1996).
4. A. D. Cucchi Colleoni, J. I. Carreto, "Variación estacional de la biomasa fitoplanctónica en el golfo San Jorge. Resultados de las campañas de investigación: OB-01/00, OB-03/ 00, OB-10/00, y OB-12/00", (Informe Técnico Interno N°49, 2001).
5. J. I. Carreto *et al.*, in Carreto, J.I., Bremec, C. Eds., El Mar Argentino y sus recursos Pesqueros, El ambiente Marino Tomo V, (INIDEP, Mar del Plata, 2007).
6. M. Fernández, A. Roux, E. Fernández, J. Caló, A. Marcos, H. Aldacur, Grain-size analysis of surficial sediments from Golfo San Jorge, Argentina. *J. Mar. Biol. Assoc. UK*, **83**, 1193–1197 (2003).
7. M. Fernández, Características físico-químicas de los sedimentos del golfo San Jorge y su relación con los organismos bentónicos del sector, PhD. thesis, Universidad Nacional de Mar del plata, Facultad de Ciencias Exactas, Argentina (2006).
8. L. Rivas, J. P. Pisoni, Identification, characteristics and seasonal evolution of surface thermal fronts in the Argentinean, Continental Shelf. *J. Mar. Sys.*, 79, 134-143 (2010).
9. N. G. Glembocki, G. N. Williams, M. E. Góngora, D. A. Gagliardini, J. M. L. Orensanz, Synoptic oceanography of San Jorge Gulf (Argentina): A template for Patagonian red shrimp (Pleoticus muelleri) spatial dynamics, *Journal of Sea Research* **95**, 22-35 (2015).
10. E.M. Acha,, H.W. Mianzan, R.M. Guerrero, M. Favero, J. Bava, Marine fronts at the continental shelves of austral South American physical and ecological processes. *J. Mar. Syst.* **44**, 83–105 (2004).

11. L. Rivas, A. I. Dogliotti, D. A. Gagliardini, Seasonal variability in satellite-measured surface chlorophyll in the Patagonian Shelf. *Cont. Shelf Res.*, **26**, 703–720 (2006).
12. S. I. Romero, A. R. Piola, M. Charo, C. A. E., Garcia, Chlorophyll-a variability off Patagonia based on SeaWiFS data. *Journal of Geophysical Research*, **111**, C05021 (2006).
13. M. Fernández, M., J. I. Carreto, J. Mora, A. Roux, Physico-chemical characterization of the benthic environment of the golfo San Jorge, Argentina. *J. Mar. Biol. Assoc. UK*, **85**, 1317–1328 (2005).
14. M. Fernández, J. Mora, A. Roux, A. D. Cucchi-Colleoni, J. C. Gasparoni, New contribution on spatial and seasonal variability of environmental conditions of the golfo San Jorge benthic system, Argentina. *J. Mar. Biol. Assoc. UK* **88**, 227–236 (2008).
15. Krock et al., 2015; B. Krock, C. M. Borel, F. Barrera, U. Tillmann, E. Fabro, G. O. Almandoz, M. E. Ferrario, J. E. Garzón Cardona, B. P. Koch, C. Alonso, R. J. Lara, Analysis of the hydrographic conditions and cyst beds in the San Jorge Gulf, Argentina, that favor dinoflagellate population development including toxigenic species and their toxins, *Journal of Marine Systems*, **148**, 86-100 (2015).
16. B. G. Mitchell, M. Kahru, J. Wieland, M. Stramska, "Determination of spectral absorption coefficients of particles, dissolved materials and phytoplankton for discrete water samples" (in Ocean Optics Protocols for Satellite Ocean Color Sensor Validation, Revision 4, vol. 4, Inherent Optical Properties: Instruments, Characterization, Field Measurements and Data Analysis Protocols, NASA Tech. Rep. 2003-211621, edited by J. L. Mueller, G. S. Fargion, and C. R. McClain, pp. 39–64, Goddard Space Flight Cent., Greenbelt, Md., 2003).
17. C. M., Yentsch, Measurement of visible light absorption by particulate matter in the ocean. *Limnology and Oceanography*, **7**, 207–217 (1962).
18. B.G. Mitchell, Algorithms for Determining the Absorption Coefficient of Aquatic Particulates Using the Quantitative Filter Technique (QFT). *Ocean Optics*, **vol. X**. 137–148 (1990).
19. M. Kishino, M. Takahashi, N. Okami, S. Ichimura, Estimation of the spectral absorption coefficients of phytoplankton in the sea. *Bulletin of Marine Science*, **37 (2)**, 634–642 (1985).
20. M. Babin, D. Stramski, Light absorption by aquatic particles in the near-infrared spectral region, *Limnol. Oceanogr.* **47(3)**, 911–915 (2002).
21. J. D. H. Strickland, T. R. Parsons, "A Practical Handbook of Seawater Analysis" (Second Edition. Bulletin 167. Fisheries Research Board of Canada, Ottawa 311 pp. ( 1972).
22. B. H. McArdle, 1988, The structural relationship: regression in biology. *Canadian Journal of Zoology*, **66**, 2329–2339 (1988).
23. R. Sokal, F. J. Rohlf, Biometry. (W.H. Freeman and Company, New York 408 pp., 1995).

- 24.** Campbell, 1995; J. W. Campbell, The lognormal distribution as a model for bio-optical variability in the sea. *Journal of Geophysical Research* **100**, 13237–13254 (1995).
- 25.** K. L. Carder, F. R. Chen, J. P. Cannizzaro, J. W. Campbell, B. G. Mitchell, Performance of the MODIS semi-analytical ocean color algorithm for chlorophyll-a. *Advances in Space Research* **33**, 1152–1159 (2004).
- 26.** Morel, L. Prieur, Analysis of variations in ocean color. *Limnology and Oceanography*, **22**, 709–722 (1977).
- 27.** H. R. Gordon, A. Morel, "Remote assessment of ocean color for interpretation of satellite visible imagery: a review" (Lecture Notes on Coastal and Estuarine Studies, vol. 4. Springer, New York, p. 114, 1983).
- 28.** J. E. Chaves, P. J. Werdell, C.W. Proctor, A. R. Neeley, S. A. Freeman, C. S. Thomas, S. B. Hooker. Assessment of ocean color data records from MODIS-Aqua in the western Arctic Ocean. *Deep-Sea Research Part II: Topical Studies in Oceanography*, 118, 32-43 (2015).
- 29.** G. H. Tilstone, A. A. Lotliker, P. I. Miller, P. Muhamed Ashraf, T. Srinivasa Kumar, T. Suresh, B. R. Ragavan, H. I B. Menon, Assessment of MODIS-Aqua chlorophyll-a algorithms in coastal and shelf waters of the eastern Arabian Sea. *Continental Shelf Research*. **65**, 14–26, (2013).
- 30.** P. Minu, A. A. Lotliker, S.S. Shaju, P. Muhamed Ashraf, T. Srinivasa Kumar, B Meenakumari, Performance of operational satellite bio-optical algorithms in different water types in the southeastern Arabian Sea. *Oceanologia*, *In press* (2015).
- 31.** Lee et al., 1998; Z. Lee, K. L. Carder, C. D. Mobley, R. G. Steward, J. S. Patch, J. S. Hyperspectral remote sensing for shallow waters. I. A semi-analytical model. *Applied Optics*, **37** (27), 6329–6338 (1998).
- 32.** K. L. Carder, F. R. Chen, Z. P. Lee, S. K. Hawes, Semianalytic moderate resolution imaging spectrometer algorithms for chlorophyll a and absorption with bio-optical domains based on nitrate-depletion temperatures, *J. Geophys. Res.*, **104**(C3), 5403–5421 (1999).



**Figure 1.** Study area and location of the stations sampled during the Coriolis R/V Oceanographic cruise in Summer 2014 overlaying a MODIS Aqua daily image (February 12, 2014). The grey contour indicates the area of San Jorge fronts mean location (adapted from Glembocki et al., 2015 (9))



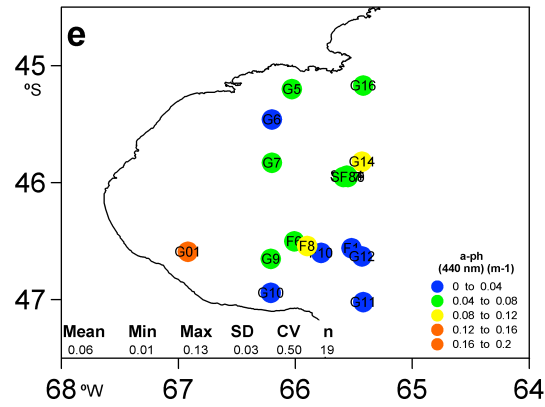


**Figure 2.** Spatial distribution of (a) Chl-a (red circles: data used in the  $\pm 3$ h time window match-up), (b) CDOM (440 nm), (c)  $a_p$  (440 nm), (d)  $a_d$  (440 nm) and (e)  $a_{ph}$  (440 nm).

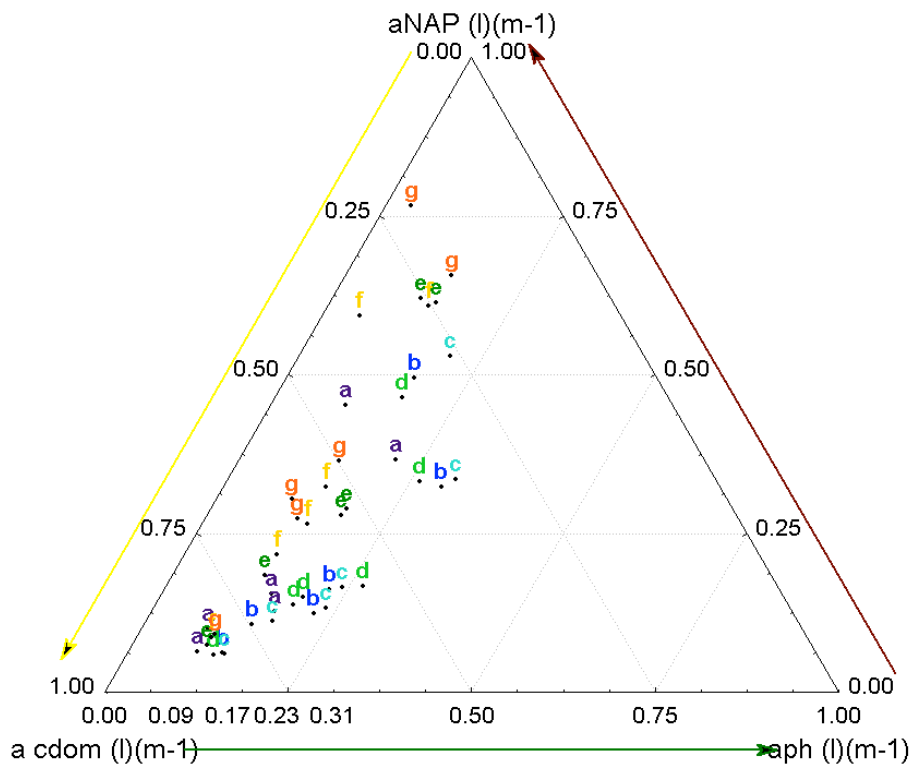


**Figure 3.** Ternary plots illustrating the relative contribution of surface phytoplankton, NAP, and CDOM to total non-water absorption at seven MODIS wavelengths (a: 412 b:443 c:469 d:488 e:531 f:547 g:555 (n=8)).

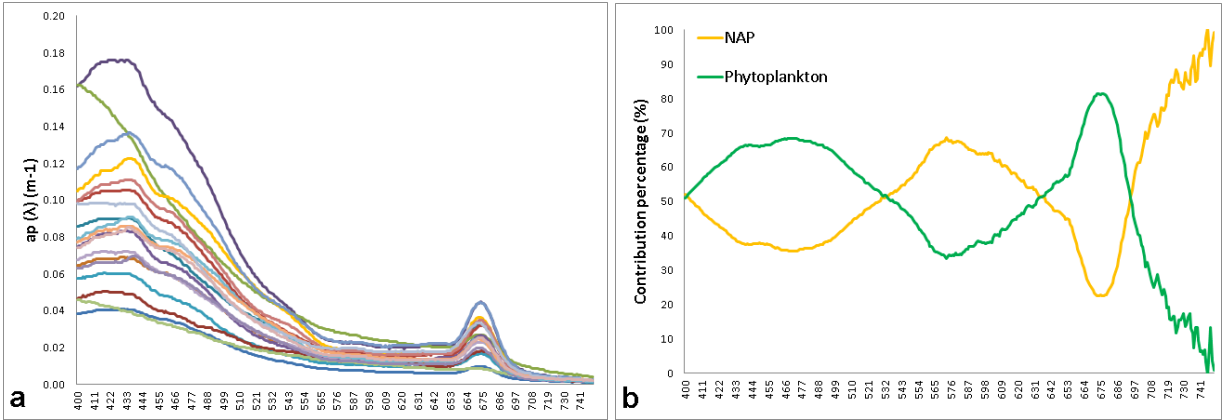


**Figure 4.** (a) Particle absorption spectra ( $a_p(\lambda)$ ) and (b) percent contribution of NAP and phytoplankton to  $a_p(\lambda)$  at the surface ( $n=19$ ).

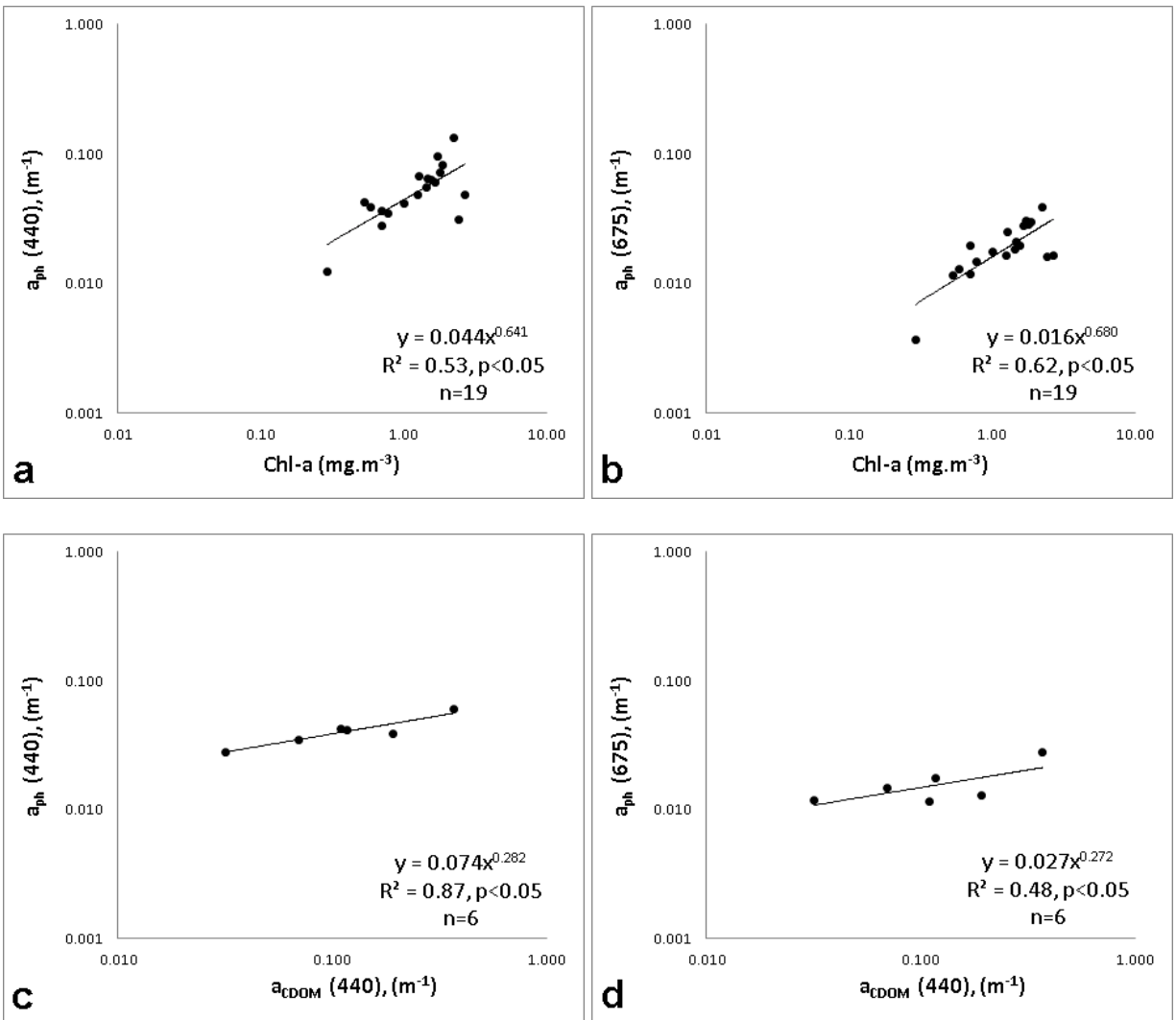


**Figure 5.** Scatterplots of (a) Chl-a versus  $a_{ph}(440)$ , (b) Chl-a versus  $a_{ph}(675)$ , (c)  $a_{CDOM}(440)$  versus  $a_{ph}(440)$  and (d)  $a_{CDOM}(440)$  versus  $a_{ph}(675)$ .

**Table 1.** Statistical results of the OC3M algorithm comparison. Linear correlation was statistically significant ( $p < 0.05$ ).

<b>selected Time window</b>	<b>Maximum time difference</b>	<b>S</b>	<b>I</b>	<b>n</b>	<b>r<sup>2</sup></b>	<b>p</b>	<b>RPD</b>	<b>RMSE</b>	<b>APD</b>	<b>rmse-log</b>	<b>rmse-L</b>
20 h	19 h	0.79	-0.036	18	0.34	0.012	26.72	68.1	50.4	0.24	2.04
12 h	8h	0.90	-0.046	14	0.46	0.008	26.22	65.0	48.1	0.23	2.00
6 h	5h	0.79	-0.032	11	0.43	0.029	25.30	68.8	50.0	0.25	2.11
3h	3h	1.00	-0.091	7	0.89	0.010	25.77	28.2	19.5	0.10	1.14

S= slope, I= intercept,